QUANTUM MECHANICAL MODEL AND SIMULATION OF GaAs/AlGaAs QUANTUM WELL INFRARED PHOTODETECTOR- II ELECTRICAL ASPECTS

Fu Y   Willander M

(Physical Electronics and Photonics, Microtechnology Center at Chalmers, Department of Microelectronics and Nanoscience, Chalmers University of Technology, Fysikgränd 3, S - 412 96 Gothenburg, Sweden)

LI Ning   LU W

(National Laboratory for Infrared Physics, Shanghai Institute of Technical Physics, Chinese Academy of Sciences, 500 Yutian Road, Shanghai 200083, China)

Abstract   A complete quantum mechanical model for GaAs/AlGaAs quantum well infrared photodetectors(QWIPs) was presented. The photocurrent was investigated by the optical transition(absorption coefficient)between the ground state and the excited states due to the nonzero component of the radiation field along the sample growth direction. By studying the inter-diffusion of the Al atoms across the GaAs/AlGaAs heterointer faces, the mobility of the drift-diffusion carriers in the excited states was calculated. As a result, the measurement results of the dark current and the photocurrent spectra are explained theoretically.

Key Words   quantum well infrared photodetector(QWIP), inter-diffusion, carrier mobility, alloy scattering, wavefunction boundary condition.

Introductdon

In the first part, we have discussed the opitical aspects about the quantum well infrared photodetector. Here we continue discussions about the electrical aspectes of the device model and simulation.

1   Dark Current and Photocurrent

Distributed effects of external bias across the system began recently to attract attentions[1,2]. Since the barrier regions are normally undoped and in general, the carrier concentration in the barrier region can be neglected, the electric field there can be well approximated as constant, as assumed in many theoretical analyses[3,4]. The electric field in each quantum well is negligible as compared with the ones in the barriers because of the high density of free carriers and the coincidental spatial distributions of electrons in the quantum well with the doped impurities[5].

We continue considering the QWIP system consisting of 50 periods of 50-nm-$Al_{0.3}Ga_{0.7}As$/5-nm-GaAs. Generally speaking, due to the surface kinetic processes, a certain degree of GaAs and AlGaAs intermixings is inevitable at the heterointerface[6]. The intermixing is enhanced by postgrowth treatments[7~14]. The GaAs/AlGaAs heterointerfaces are described by the degree of the Al inter-diffusion[15~17]

$$x(z) = \frac{x_0}{2}\left[2 + \text{erf}(\frac{z - dw/2}{2L}) - \text{erf}(\frac{z - dw/2}{2L}) \right], \tag{1}$$

where x_0 is the initial Al concentration in the barrier, dw the quantum well width, L the diffusion length, and erf the error function. The center of the well locates at $z = 0$.

The diffusion length is determined by matching the values of the cutoff wavelength obtained theoretically and experimentally. Typical measurement data of photocurrent spectra are presented in Fig. 1. By fitting the

peak position of 7. 85μm (0. 158eV) for the as-grown QWIP sample in Fig. 1 , an Al diffusion length of 2. 9 Å is obtained. At this moment, there is one sublevel E_0 confined in the quantum well which is 0. 158eV below the AlGaAs conduction bandedge, the local Fermi level E_f is 7 meV above E_0 at 77K. Thus the xy-plane kinetic energies of carriers are neglected in the following discussion

Fig. 2 shows very small occupation probability $f(E_k)$ of excited states E_k above the barriers (the Al-GaAs conduction bandedge is zero). On the other hand, the electron transport from one quantum well to the next quantum well is in the contest of coherent wave transmission [18,19]

$$\varphi_k(z) = e^{ikz} + re^{-ikz},\qquad(2)$$

in the quantum well that emits the electron wave,

$$\varphi_k(z) = t_k e^{ikz},\qquad(3)$$

in the quantum well that collects the transmission wave. Here the QWIP is not biased. $\hbar^2 k^2/2m^* = E_k$. The transmission probability $|t_k|^2$ as a function of E_k is plotted in Fig. 2 , showing that due to the thick barriers the escape of carriers occupying the ground state E_0 in one quantum well to the next is almost impossible. By the complex eigenvalue approach it was concluded[20] that the lifetime of the electrons in the localized ground state E_0 is rather long so that these carriers have a rather small rate to escape to the adjacent wells through barriers.

By Fig . 2 it is observed that in the QWIP system, thermal excitation dominates. In other words, the dark current consists of mainly thermally excited carriers o-
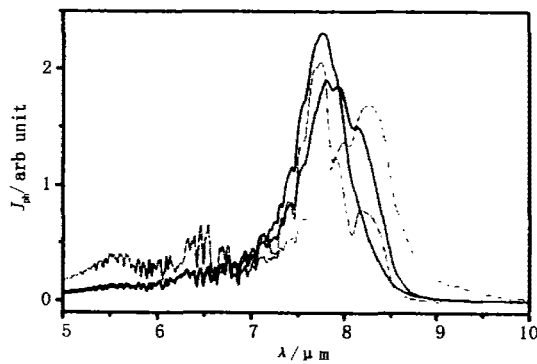
ver the barriers. It is also reconfirmed here that the current density is rather low so that the approximation of quas-iequilibrium state is well established (we have used such an approximation by introducing the Fermi level E_f). The approximation of the nonconductive QWIP system when discussing the propagation of the e-lectromagnetic field (in the first part) is also established due to this low conduction current.

It is concluded that electrons in one quantum well transmit to other spatial regions (adjacent quantum wells and contacts) via thermal activation above the barrier(forming the dark current), they become photo-excited to excited states above the barrier by the incident infrared radiation(forming the photocurrent). The current density has been modeled as $J = ev_d n'$ [3,4, 21,22], where v_d is the carrier drift velocity

$$v_d = \mu F_z \left[1 + (\frac{\mu F_z}{v_s})^2 \right]^{-1/2},\qquad(4)$$

v_s is the saturation drift velocity ranging from 0. 1 × 10^6 to 5 × 10^6 cm/s, μ is the low-field carrier mobility (2000cm²/V · S for n-type AlGaAs QWIPs) , and F_z is the electric field intensity in the barrier region induced by the external bias. The density of mobile carriers n' in the quantum well consists of two parts, $n' = n'_{th} + n'_{ph}$, where n'_{th} is the carrier density due to the thermal excitation

$$n'_{th} = \int_{E_z \geq 0} \frac{2dkdk}{(2\pi)^3} f(E_k, k),\qquad(5)$$

It is easy to see that in general, the optical transition probability is very small so that the carrier distri-

Fig. 1 Photocurrent J_{ph} spectra of our QWIP dvices at 77K.
From the highest to the lowest spectrum
the ion implantation doses are 0. 0,0. 7,
1. 0 and 5 × 10^15 cm^-3

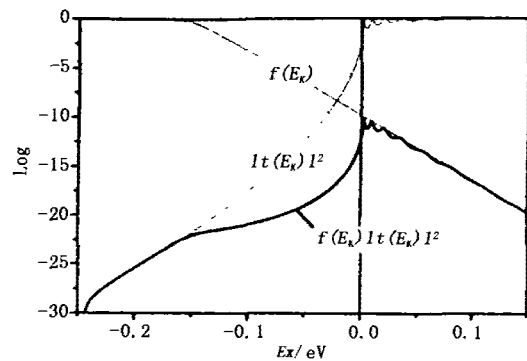Fig. 2 Occupation probability and transmission from
one quantum well to the next as functions of the electron
energy in the z-direction(the wave vector in the
xy-plane is zero)
$L = 2.9$ A, $E_0 = -0.158$eV, $E_f = -0.151$eV at 77K

bution of the ground state is almost unchanged. The photonexcitation is

$$n'_{ph} = n_0 \int \langle \ | \ A_z(\hbar\omega) \ | \ ^2 \rangle \mathrm{d}(\hbar\omega) \int \frac{2\mathrm{d}k}{2\pi}$$

$$\left| \left\langle \varphi_k \left| \frac{eh}{m^*} \frac{\partial}{\partial z} \right| \varphi_0 \right\rangle \right|^2 \frac{\Gamma}{(E_k - E_0 - \hbar\omega)^2 + \Gamma^2}, \quad (6)$$

where n_0 is the carrier density occupying the ground state (E_0, φ_0).

Normally the QWIP is calibrated with blackbody. The optical spectrum from the blackbody is obtained by the Planck's formula

$$n_{ph}(\hbar\omega) \propto \frac{\omega^4}{e^{\hbar\omega/k_B T_b} - 1}, \quad (7)$$

where T_b is the temperature of the blackbody.

Theoretical results of the absorption coeffcient, photocurrent and dark current density of our QWIP samples are presented in Fig. 3. Here $L = 2.9$ Å, the device temperature is 77K, and the blackbody calibration temperature is 500K. Comparing the absorption and photocurrent spectra, it is observed that the short wavelength absorption is suppressed by the blackbody optical spectrum of Eq. (7). The calculated photocurrent density fits quite well with the measurement data of Fig. 1 in the first part, except that the theoretical value of the saturation current density is about 2 times smaller than the measurement. The discrepancy is expected as we neglect leakage currents, e. g. , the leakage current at the mesa edge. The asymmetric I-V characteristics with respect to the external bias is due to the asymmetric quantum wells (we can expect gradual decrease/increase of the Al content at the beginning/end of quantum well growth in a normal MBE growth man-
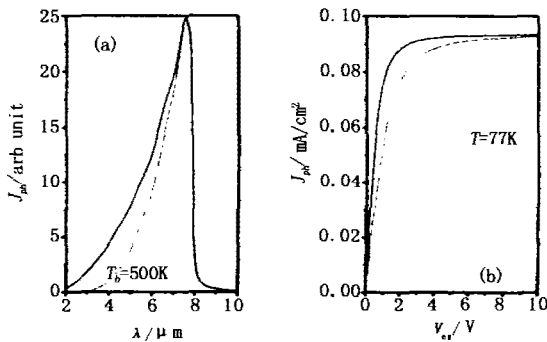

Fig. 3. (a) Calculated absorption(solid line) , photocurrent(dotted line) and (b) dark current density. Solid lines: $\mu = 2000$; dotted lines: $\mu = 1000 \mathrm{cm}^2/\mathrm{V. s.}$

ner)

2 Boundary Conditions of Continuum States

We consider the multiple quantum well structure in the form of $V[z + n(\mathrm{d}_B + \mathrm{d}_W)] = V(z)$, where

$$V(z) = \begin{cases} \triangle E_c, & -\mathrm{d}_W/2 - \mathrm{d}_B \leqslant z < -\mathrm{d}_W/2 \\ 0, & -\mathrm{d}_W/2 \leqslant z < \mathrm{d}_W/2 \\ \triangle E_c, & \mathrm{d}_W/2 \leqslant z < \mathrm{d}_W/2 + \mathrm{d}_B \end{cases}, \quad (8)$$

n is an integer, d_B is the AlGaAs barrier width, and $\triangle E_c$ is the barrier height. There is one localized state confined in the GaAs quantum well and its boundary conditions are unambiguous that the corresponding wave function is zero deep inside the AlGaAs barriers. It is consistent numerically with other theoretical considerations, e. g. , the complex eigenvalue approach[20,23~25]. Theoretically there exist three types of boundary conditions for extended states. In early works [26~29], the GaAs quantum well and its adjacent two AlGaAs barriers were approximately embedded in an infinitely high barrier media, which is denoted this as a box approximation. Because of the infinitely high barrier at the two ends, extended states above the AlGaAs barrier becomes discrete and are denoted as $E_i, i = 1, 2, \cdots\cdots$ Knowing the wave functions it is then easy to calculate the optical matrix element of $< \varphi_i \ | \ \partial/\partial_z \ | \ \varphi_0 >$. The separations between E_i and E_0, $E_i - E_0$ and the matrix elements are shown in Fig. 4 as the dotted line.

However, due to the consideration of the carrier transport in the QWIP under normal device working conditions, we must envisage the condution of both the thermal-excited and photo-excited electrons from one quantum to the next one. We first consider the running wave

$$\psi_{\text{running}}(z) = \begin{cases} e^{ikz} + re^{-ikz}, & z < -\mathrm{d}_W/2 \\ Ae^{iqz} + Be^{-iqz}, & -\mathrm{d}_W/2 \leqslant z < \mathrm{d}_W/2, \\ te^{ikz}, & z \geqslant \mathrm{d}_W/2 \end{cases} \quad (9)$$

for $E > \triangle E_c$. Here

$$\frac{\hbar^2 q^2}{2m^*} = E - \triangle E_c, \quad \frac{\hbar^2 k^2}{2m^*} = E, \quad (10)$$

The corresponding optical matrix elements are presented in Fig. 4 as curve A which is rather smooth for

states with E less than 0. 1 eV above the AlGaAs barrier. A peak appears at about $E = 0.12$eV and then the matrix element is basically zero. The results are understood by the parity of wave functions which shows that in the region of the quantum well(in the present case, $z \in (-25, 25)$Å), the wave functions below 0. 1eV are odd. They become even when E is about 0. 13eV above the barrier.

The third alternative is the transport of the excited continuum states in the Bloch wave form

$$\psi_{Bloch}(z) = u(z)e^{iKz}, \qquad (11)$$

where $u(z) = u[z + n(d_W + d_B)]$ accounts the periodic boundary conditions of the GaAs/AlGaAs multiple quantum wells. The corresponding optical matrix element is presented in Fig. 4. We can see a close similarity between this approach and the box approach except that some peaks and valleys are missing in the box approach.

Knowing the optical matrix elements, the optical absorption spectra are easily calculated and numerical results are presented in Fig. 5. Fine structures were observed experimentally in QWIPs consisting of multiple quantum wells, whereas single-quantum-well QWIPS display simple spectra[30]. Fig. 5 suggests the Bloch-state boundary conditions as the most proper ones for continuum states in characterizing QWIPs consisting of multiple quantum wells(the discrepancy between the theoretical and experimental spectra at low wavelength range can be the results of the complicated conduction band structure at higher electron energies,
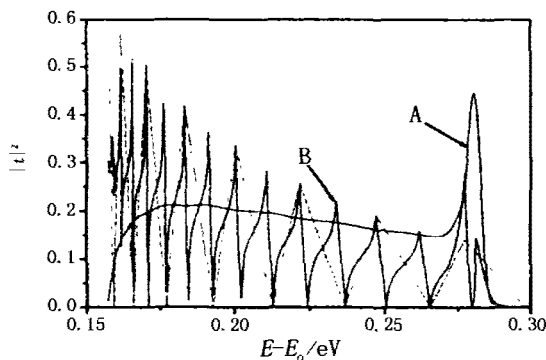
where the simple effective mass approximation is not valid), the boundary conditions of running waves are definitely proper for QWIPs consisting of a single quantum well or only a few quantum wells, as demonstrated by the tunneling effect experimentally[31].

3 Alloy Scattering and Carrier Mobility

Recently researchers have been interested in the application of quantum well intermixing techniques [8,11] to modify energy levels of heterosystems. The ion implantaion using materials such as Si[7], As[10] and then further encapsulation by a dielectric layer such as SiO_2 and Si_3N_4 have been proven to be rather effective.

Figure 6 shows dark current spectra from annealed and ion-implanted QWIP samples. Note that the dark current increases by nearly a factor of 2 after proton implantation while it is almost unchanged after annealing. Fig. 1 shows the photocurrent spectra at a negative bias of about-3V. Peak response wavelengths are 7. 76 ,7. 87 and 8. 28μm for the as -grown, and samples implanted with H$^+$-dose 1 × and 2. 5 × 10^{15} cm^{-3}, respectively. Theoretically it is expected that due to the ion implantation and annealing, the Al atoms diffuse from barrier regions into well regions. The bottom of the quantum well is lifted up and the width of the quantum well is effectively reduced so that subband energies of carriers are increased.

The Al diffusion length is determined by matching the peak positions of the theoretical absorption and experimental photocurrent spectra. Numerical results of the Al diffusion length are listed in Table I. It is concluded by fitting the peak positions that the Al diffusion

Fig. 4/Optical matrix element as a function of the energy separation between the extended state and the bound state. Curve A: running wave; Curve B: Bloch wave. Dotted line: box approximation
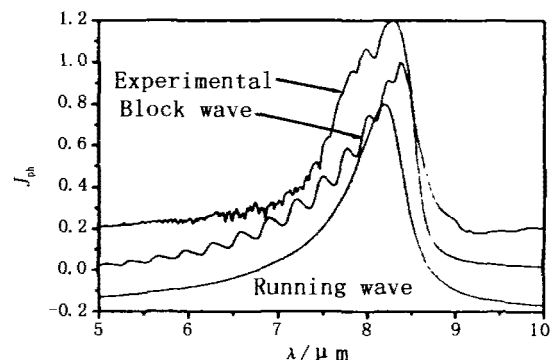
Fig. 5 Calculated optical absorption rates and a typical photocurrent spectrum of QWIP measured at 77 K

length increases from 2.9 to 6.5 Å when the dose of the ion-implantation increases up to $2.5 \times 10^{15} cm^{-3}$. In addition to the redshift of the absorption peak we have observed an increased absorption intensity following the increase of the Al diffusion length. It is due to the increased coupling between the ground state and excited states when the energy separation between them decreases. However the photocurrent decreases experimentally following the increased H^+ dose.

On the other hand, the density of thermally excited carriers increases by a factor of 4.6 when L increases from 2.9 to 6.5 Å, while experimentally the dark current increases by a factor of only 2. It must thus be concluded that we have to take into account the microscopic mechanism(which has reduced the carrier lifetime) when studying the carrier trasnsport property. Postgrowth processes enhance various scatterings so that the lifetime of carriers at excited states is reduced, and the absorption coefficient is therefore decreased. The concept of carrier lifetime is introduced for steady states. In studying the carrier transport we consider unperturbed electronic states and the transport properties of carriers occupying these states are perturbed by various scattering centers. At the normal QWIP device working temperature of 77K, alloy scattering is expected to be dominant in GaAs/AlGaAs-based materials. Phonon and impurity scatterings are limited due to the low device working temperature and spatially localized doping profile.

We consider a ternary compound $A_x B_{1-x} C$, where the mole fraction x of atom A varies along the sample
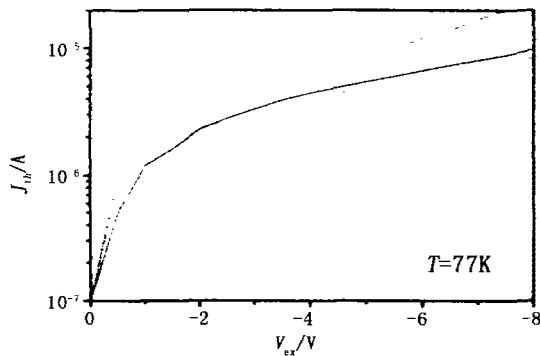

Fig. 6   Dark currents spectra of an as-grown QWIP sample(solid line) , annealed (dotted line) and ion-implanted with H^+ dose of $2.5 \times 10^{15} cm^{-3}$ (dashed line)

growth direction (z-direction) so that $x = x(z)$. Now the potential energy $V(r)$ for the one-electron Schrodinger equation is divided into a virtual crystal part

$$V_0(r) = \sum_a [xV_A(r-a) + (1-x)V_B(r-a)] , \quad (12)$$

and a random potential part

$$V'(r) = \sum_a c_a [V_A(r-a) - V_B(r-a)] , \quad (13)$$

where $V_A(r-a)$ and $V_B(r-a)$ are periodic atomic potentials of compound AC and BC, c_a is a random function which is defined only at lattice site a,

$$c_a = \begin{cases} (1-x) & \text{for an A atom at } a \\ -x & \text{for a B atom at } a \end{cases}, \quad (14)$$

The total scattering rate of state ik [32]

$$M(ik) = \triangle^2 [1 - f(E_{ik})] \int [1 - x(z)]x(z)\varphi_i(z) \mid^4 dz , \quad (15)$$

The velocity relaxation time associated with alloy scattering is

$$\frac{1}{\tau(ik)} = \frac{2\pi\triangle^2}{h}[1 - f(E_{ik})] \int [1 - x(z)]x(z) \mid \varphi_i(z) \mid^4 dz, \quad (16)$$

The above expression reduces to the ones of Ando[33] Bastard[34] when the alloy composition is constant in the barrier region. It further reduces to the one of bulk material when the alloy composition is constant in the whole sample, e. g. , see Ref. [35].

The mobility μ_z along the z-direction determined by the alloy scattering becomes then

$$\mu_z = \frac{e}{n'} \int \frac{2dK}{(2\pi)^3} \tau(K) v_z^2(K) \frac{\partial f(E_K)}{\partial E_K}, \quad (17)$$

where $K = (\kappa, k)$, κ is the wave vector in the xy plane. $hv_z = \partial E_K / \partial k$. Increasing L from 2.9 to 6.5 Å (corresponding to the H^+ dose of $2.5 \times 10^{15} cm^{-3}$) , the calculated mobility decreases from 0.82 to 0.33, a factor of 2.5. We then expect an increasing factor of $31.978 \times 0.33/(6.875 \times 0.82) = 1.8$ in the dark current, which agrees very well with Fig. 1 in the first part of this article, where a factor about 2.0 has been observed. For the photocurrent, it is 0.56 v. 0.65. Detailed data are listed in Table I.

Table 1 Numerical values of physical quantities

H$^+$ dose[10^{15}cm^{-3}]	0	2.5	Exp.
Diffusion length L Å	2.9	6.5	
Peak absorption coefficient	24.75	34.61	
n'_{th}[10^7cm^{-3}]	6.875	31.978	
Carrier mobility	0.82139	0.32895	
Dark current	1	1.8	2.0
Peak photocurrent	1	0.56	0.65

4 Summary

It has thus been concluded that for n-type GaAs-AlGaAs-based quantum well infrared photodetector, (1) Optical grating is necessary because of the spherical and parabolic energy band structure of the active relectrons in the GaAs-AlGaAs material (quantum selection rule); (2) At the normal QWIP working condition (77K), electrons are largely confined in the ground states in the quantum wells. Direct tunneling effect from one quantum well to the neighboring quantum wells is negligible. The dark current of the device consists of mainly the drift-diffusion current of thermally excited carriers; (3) Photoexcitation happens between the ground state confined in the quantum well and the extended states above the barriers along the sample growth direction; (4) At normal QWIP working temperature, the transport of the thermally-excited and photocarriers is in the form of three-dimensional drift-diffusion limited by the alloy scattering due to Al atom distribution.

REFERENCES

[1] Ryzhii V. Characteristics of quantum well infrared photodetectors. *J. Appl. Phys.*, 1997, **81**: 6442 — 8

[2] Thibaudeau, L, Bois P, Duboz J Y. A self-consistent model for quantum well infrared photodetectors. *J. Appl. Phys.*, 1996, **79**: 446 — 54

[3] Andrews S R, Miller B A. Experimental and theoreticaly studies of the performance of quantum well infrared photodetectors. *J. Appl. Phys.*, 1991 **70**: 993 — 1003

[4] Whitney R L, Cuff K F, Adams F W. Chapter 3 long wavelength infrared photodetectors based on intersubband transitions in III-V semiconductor quantum wells, *Semiconductor Quantum Wells and Superlattices for Long-Wavelength Infrared Detectors*. Boston Artech House Boston: Artech House, 1993, 55 — 108

[5] Fu Y Willander M, Lu W, et al. Optical coupling in quantum well infrared photodetector by diffration grating. *J. Appl. phys.*, 1998, **84**: 5750 — 5

[6] Madhukar A. *Physics of Quantum Electron Devices*, Berlin Springer-Verlag: 1990, 50

[7] Gavrilovic P, Deppe D G, Meehan K, et al. Implantation disordering of Al$_x$Ga$_{1-x}$As supperlattices. *Appl. Phys. Lett.* 1985, **47**: 130 — 2

[8] Elman B, Koteles E S, Melman P. GaAs/AlGaAs quantum well intermixing using shallow ion implantation and rapid thermal annealing. *J. Appl. Phys.*, 1989, **66**: 2104 — 7

[9] Chi J Y, Wen X, Koteles E S, et al. Spatially selective modification of GaAs/AlGaAs quantum wells by SiO capping and rapid thermai annealing. *Appl. Phys. Lett.*, 1989, **55**: 855 — 7

[10] Steele A G, Buchanan M, Liu H C. et al. Postgrowth tunning of quantum well infrared detectors by rapid thermal annealing. *J. Appl. Phys.*, 1994, **75**: 8234 — 6

[11] Tan H H, Williams J S, Jagadish C, et al. Large energy shifts in GaAs-AlGaAs quantum wells by proton irradiation-induced inter mixing. *Appl. Phys. Lett.*, 1996, **68**: 2401 — 3

[12] Yuan S, Kim Y, Tan H H, et al. Anodic-oxide-induced interdiffusion in GaAs/AlGAaAs quantum wells. *J. Appl. Phys.*, 1998, **83**: 1305 — 11

[13] Li Ning, Fu Y, Karlsteen M, et al. Fine structures of photo-response spectra in quantum well infrared photodetector. *Appl. Phys. Lett.*, 1999, **75**: 2238 — 40

[14] Li Na, Li Ning, Lu we, et at. Proton implantation and rapid thermal annealing effects on GaAs/AlGaAs quantum well infrared photodetector. *Superlattices and Microstructures*, 1999, **26**: 317 — 24

[15] Crank J. *The Mathematics of Diffusion*, Oxford: Clarendon 1956

[16] Redinbo G F, Craighead H G, Hong J M. Proton implantation intermixing of GaAs/AlGaAs quantum wells. *J. Appl. Phys.* 1993, **74**: 3099 — 102

[17] Feng W, Chen F, Cheng W Q, et al. Influence of growth conditions on Al-Ga interdiffusion in low-temperature grown AlGaAs/GaAs multiple quantum wells. *Appl. Phys. Lett.*, 1997, **71**: 1676—8

[18] Sofo J O, Balseiro C A. Intrinsic bistability in resonant tunneling structures. *Phys. Rev.*, 1990, **B42**: 7292 — 5

[19] Fu Y, Williander M. Charge accumulation and band edge in the double barrier tunneling structure. *J. Appl. Phys.*, 1992, **71**: 3877 — 82

[20] Fu Y, Li N, Karlsteen M, et al. Thermoexcited and photoexcited carrier transports in a GaAs/AlGaAs quantum well infrared photodetecor. *J. Appl. Phys.*, 2000, **87**: 511 — 6

[21] Levine B F, Bethea G C, Hasnain G, et al. High sensitivity low dark current 10 GaAs quantum well infrared photodetector. *Appl. phys. Lett.*, 1990, **56**: 851

[22] Williams G M, DeWames R E, Farley C W, et al. Excess tunnel currents in AlGaAs/GaAs mulitiple quantum well infrared detectors. *Appl. Phys. Lett.*, 1992, **60**: 1324 — 6

[23] Bahder T B, Morrison C A, Bruno H D. Resnant level lifetime in GaAs/AlGaAs double-barrier structures. *Appl. Phys. Lett.*, 1987, **51**: 1089 — 90

[24] Buno J D, Bahder T B, Morrison C A. Limiting response time of double-barrier resonant tunneling structures. *Phys.*

Rev. ,1988,B37:7098 — 101

[25]Zou N, Rammer J, Chao K A. Tunneling escape of electrons from a double-barrier structure. *Phys. Rev.* , 1992, B46: 15912 — 21

[26]Ikonic Z, Milanovic V, Tjapkin D. Bound-free intraband absorption in GaAs-Al$_x$Ga$_{1-x}$ As semiconductor quantum wells. *Appl. Phys. Lett.* , 1989, **54**: 247 — 9

[27]Liu H C. Dependence of absorption spectrum and responsivity on the upper state position in quantum well intersubband photodectors. *J. Appl. Phys.* , 1994, **73**: 3062 — 7

[28] Rusli, Chong T C, Chua S K. Theoretical analysis of bound-to-continuum state infrared absorption in GaAs/All-xGaxAs quantum well structures. *Jpn. J. Appl. Phys.* , 1993, **32**: 1998 — 2004

[29]Xu W, ·Fu Y, Willander M. Oscillator strength of intersubband transition in n-type AlAs/GaAlAs quantum well for the normal incident absorption. *J. Infrared Millim Waves*,

1997, **16**: 86 — 92

[30]Levine B F. Quantumm well infrared photodetectors. *J. Appl. Phys.* , 1993, **74**: R1 — 81

[31]Bandara K M S V, Levine B F, Asom M T. Tunneeling emitter undoped quantum-well infrared photodetector. *J. Appl. Phys.* , 1993, **74**: 346 — 50

[32] Fu Y, Willander M. Alloy scattering in GaAs/AlGaAs quantum well infrared photodetector. *J. Appl. Phys.* , 2000, **88**: 288 — 92

[33] Audo T. Self-consistent results for a GaAs/Al$_x$Ga$_{1-x}$ As heterojunction. II. Low temperature mobility. Japan: *J. Phys. Soc.* 1982, **51**: 3900 — 7

[34]Bastard G. Energy level and alloy scattering InP-In(Ga)As heterojunctions. *Appl. Phys. Lett.* , 1983, **43**: 591 — 3

[35]Ridley B K. *Qquantum Processes in Semiconductors*. Oxford: Clarendon 1988, **181**